Journal of Molecular Structure 1119 (2016) 133–138

Contents lists available at ScienceDirect

Journal of Molecular Structure

journal homepage: http://www.elsevier.com/locate/molstruc

Newly designed silver coated-magnetic, monodisperse polymeric microbeads as SERS substrate for low-level detection of amoxicillin

Güneş Kibar [a], Ahmet Emin Topal [b], Aykutlu Dana [b], Ali Tuncel [a, c, *]

[a] Bioengineering Division, Hacettepe University, 06800, Ankara, Turkey
[b] UNAM Institute of Materials Science and Nanotechnology, Bilkent University, 06800, Ankara, Turkey
[c] Division of Nanotechnology and Nanomedicine, Hacettepe University, 06800, Ankara, Turkey

ARTICLE INFO

Article history:
Received 2 November 2015
Received in revised form
6 April 2016
Accepted 25 April 2016
Available online 27 April 2016

Keywords:
Surface enhanced Raman scattering
Antibiotic
Low-level detection
Ag nanoparticles
Amoxicillin

ABSTRACT

We report the preparation of silver-coated magnetic polymethacrylate core–shell nanoparticles for use in surface-enhanced Raman scattering based drug detection. Monodisperse porous poly (mono-2-(methacryloyloxy)ethyl succinate-*co*-glycerol dimethacrylate), poly (MMES-*co*-GDMA) microbeads of *ca.* 5 μm diameter were first synthesized through a multistage microsuspension polymerization technique to serve as a carboxyl-bearing core region. Microspheres were subsequently magnetized by the co-precipitation of ferric ions, aminated through the surface hydroxyl groups and decorated with Au nanoparticles via electrostatic attraction. An Ag shell was then formed on top of the Au layer through a seed-mediated growth process, resulting in micron-sized monodisperse microbeads that exhibit Raman enhancement effects due to the roughness of the Ag surface layer. The core–shell microspheres were used as a new substrate for the detection of amoxicillin at trace concentrations up to 10^{-8} M by SERS. The proposed SERS platform can be evaluated as a useful tool for the follow-up amoxicillin pollution and low-level detection of amoxicillin in aqueous media.

1. Introduction

Surface-enhanced Raman scattering (SERS) has been used as an efficient tool for the sensing of molecules in fields such as materials science, biochemistry, biosensing, catalysis chemistry and electrochemistry [1,2]. Gold, silver, copper and similar metals are typically utilized for Raman enhancement, and the surface architectures of metallic surfaces heavily influence the intensity and distribution of the SERS signal [3]. In recent years, various SERS substrates have designed in the form of nanoparticles, nanostars, nanopyramids, nanorods, and hybrid materials for identifying chemical structures of species [4–10]. Working with nanostructures is highly difficult because of coagulation and toxicological problem and not easy to follow up in the physical systems. In the case of nanostructures, the reproducibility of SERS signal is also poor because of non-uniform aggregation of these materials [11]. As such, an ideal SERS substrate should eliminate the problems associated with nanoparticle use and storage in addition to exhibiting an ideal SERS profile.

In this study, monodisperse-porous microspheres were chosen over nanoparticles for the preparation of a novel SERS substrate, primarily due to their advantage of handling [12–14]. Nanoscale roughnesses on the surface of porous microspheres are sufficient to create the local confinement in electromagnetic fields required for the SERS effect. The ends of nanorods, tips of nano-triangles and edges of nanocubes have previously been reported to exhibit such localized field enhancements, serving as “hot spots” for the enhancement of the SERS signal and potentially producing enhancement factors sufficient for the detection of single molecules [15,16]. Magnetic materials and imprinting technologies were also used in tandem with SERS-active nanoparticles for the design of optimal SERS detection systems [17–19]. Core-shell systems are especially popular for the fabrication of multi-functional magnetic SERS substrates of this type [20–23].

SERS substrates are generally tested using SERS-active dye molecules such as Rhodamine 6G and methylene blue [16,24]. Their practical use also extends to the characterization of cells, bacteria, proteins, drugs, DNA, organic pollutants and various chemical species in the present day [22,25–28]. The detection of various drugs was also performed using SERS in the past decade, and is of substantial importance due to the health and ecological risks

* Corresponding author. Bioengineering Division, Hacettepe University, 06800, Ankara, Turkey.
E-mail address: atuncel@hacettepe.edu.tr (A. Tuncel).

http://dx.doi.org/10.1016/j.molstruc.2016.04.086
0022-2860/

associated with antibiotic run-off [29].

The detection and the quantitative analysis of amoxicillin, a moderate spectrum β-lactam antibiotic, were performed at concentrations down to 1 μg/ml by SERS [30–33]. In this study, we report the fabrication of a new kind of silver-coated magnetic, porous polymer microspheres as a SERS substrate. A model SERS-active dye, methylene blue, was used as test material for the evaluation of substrate performance, while the aforementioned drug, amoxicillin and the commercial product of amoxicillin, were analyzed to sub-molar concentrations as proof-of-concept to evaluate the efficiency of the material for chemical characterization.

2. Experimental

2.1. Materials

Glycidyl methacrylate (GMA), glycerol dimethacrylate (GDMA), mono-2-(methacryloyloxy) ethyl succinate (MMES), (3-aminopropyl)triethoxysilane (APTES), ethylbenzene (EB), polyvinyl pyrrolidone K-30 (PVPK-30), tetrahydrofuran (THF), sodium dodecyl sulphate (SDS), Iron (II) chloride tetrahydrate ($FeCl_2 \cdot 4H_2O$), Iron (III) chloride hexahydrate ($FeCl_2 \cdot 6H_2O$), triethylenamine (TEA), ammonium hydroxide (NH_4OH), hydrochloric acid (HCl), formaldehyde (HCHO), silver nitrate ($AgNO_3$), chloroauric acid ($HAuCl_4$), polyvinyl alcohol (PVA, 87–89% hydrolyzed, average molecular weight 85,000–146,000 Da), sodium citrate tribasic dihydrate, toluene, methylene blue were purchased from Sigma–Aldrich. All chemicals used as received. Except benzoyl peroxide (BPO) dried in vacuum at 30 °C, was obtained from Aldrich. The initiator, 2,2′-azobisizobutyronitrile (AIBN) was crystallized from methanol, and absolute ethanol was obtained from Merck A.G., Darmstadt, Germany. Distilled deionized (DDI) water was supplied from Millipore/Direct Q-3UV water purification system. Amoxicillin was obtained from Faculty of Pharmacy at Hacettepe University. Largopen was supplied from Bilim İlaç San. ve Tic. AŞ as a commercial amoxicillin.

2.2. Synthesis of monodisperse-porous poly(MMES-co-GDMA) microbeads

Monodisperse poly (GMA) seed latex 2 μm in size was prepared by dispersion polymerization [34]. Plain poly (MMES-*co*-GDMA) microbeads were produced by a multistage shape-template polymerization technique. In the first step, the diluent EB (2.5 ml) was emulsified in DDI water (50 ml) including SDS (0.125 g) by sonication for 6 min. Poly (GMA) seed latex (1 mL, solid content 0.3 g) was added into this emulsion and sonicated for 6 min. The emulsion was magnetically stirred at room temperature for 24 h. Next, the functional monomer (MMES, 1.0 g), the crosslinking agent (GDMA 5.0 mL) and the initiator (BPO, 0.25 g) was mixed together and added into DDI water (50 mL) including SDS (0.125 g). The monomer phase was emulsified by sonication for 5 min. The second emulsion was then poured into the first emulsion containing swollen seed particles. The final emulsion was stirred at magnetically at room temperature for 24 h. Aqueous PVA solution (10 mL, 8% wt/wt) was added into the final emulsion and the resulting dispersion was left at 80° C in a shaking water-bath at 120 cpm for 24 h. Monodisperse-porous poly (MMES-*co*-GDMA) microbeads were isolated by successive centrifugation and decantation steps and washed respectively by EtOH, THF, EtOH several times to remove the unreacted monomers and poly (GMA) template.

2.3. Magnetization of monodisperse-porous poly(MMES-co-GDMA) microbeads

The magnetization of microbeads was performed according to the literature [35]. Typically, 1 g of poly (MMES-*co*-GDMA) microbeads were dispersed in 50 mL of DDI water. The dispersion was placed in an ice-bath under nitrogen atmosphere. 0.268 g of $FeCl_2 \cdot 4H_2O$ and 0.4 g $FeCl_2 \cdot 6H_2O$ was dissolved in 10 ml DDI water in N_2 atmosphere. The mixed salt solution was added into the dispersion containing polymer microbeads and the ice-bath was removed. The medium was evacuated till no air bubble was observed. Then a light brown mixture was formed and immediately immersed in a water-bath at 85° C. 12.5 ml of NH_4OH (25% wt/wt) was added into this mixture and the color was changed into black. The resulting dispersion was mechanically stirred at 85° C for 1 h and then cooled to room temperature. The magnetic poly (MMES-*co*-GDMA) microbeads were separated from the liquid part with a magnet and washed by DDI water and 0.1 M HCl.

2.4. Amine functionalization of magnetic-poly(MMES-co-GDMA) microbeads

Primary amine groups were attached onto magnetic poly (MMES-*co*-GDMA) microbeads via the reaction between the hydroxyl groups of magnetic microbeads and triethoxysilane groups of APTES. For this purpose, 0.5 g of dry, magnetic poly (MMES-*co*-GDMA) microbeads were redispersed in toluene (20 ml). Then 4 ml of APTES and 0.3 ml TEA was added into this mixture. The resulting dispersion was refluxed for 6 h. Amine functionalized magnetic microbeads were separated from reaction medium by a magnet and washed with ethanol several times.

2.5. Gold decoration of primary amine functionalized magnetic-poly(MMES-co-GDMA) microbeads

Frens's method was applied for gold decoration of primary amine functionalized magnetic-poly (MMES-*co*-GDMA) microbeads [36]. For this purpose, 0.02 g $HAuCl_4$ was dissolved in 24 ml DDI water and heated up to boiling under magnetic stirring. 0.07 g sodium citrate tribasic dihydrate in 1 ml water was added into boiling gold solution. The solution was kept for 10 min at boiling point until the color changed from light yellow to dark red. Then the solution was left for cooling at room temperature. After cooling down, 25 mg of primary amine functionalized magnetic-poly (MMES-*co*-GDMA) microbeads were added into gold solution under mechanical stirring. The solution was mechanically stirred at room temperature for 6 h for the attachment of gold nanoparticles onto the primary amine functionalized magnetic polymer microbeads. The gold nanoparticle decorated microbeads were separated by a magnet and washed with DDI water several times.

2.6. Growth of silver shell on gold decorated-magnetic polymer microbeads

Silver shell growth protocol in Wang's study was modified as follows [14]. 0.3 g $AgNO_3$ and 0.025 g sodium citrate tribasic dihydrate were dissolved in 25 ml DDI water by ultrasonication for 5 min. After adding 25 mg of gold decorated magnetic microbeads, pH was set to 10 by using 1 M ammonia solution. Under mechanical stirring, HCHO solution (10% wt/wt) was added into the basic dispersion and the resulting dispersion was left for 6 h for completion of the shell growth reaction. Finally, Ag shell coated magnetic beads were collected by a magnet and washed by water several times.

2.7. SERS measurements

Silver coated magnetic-polymeric microbeads were dropped onto glass slide and waited for air cooled for 5 min. Test dye MB and drugs pure amoxicillin, commercial amoxicillin solutions were prepared in different concentration (from 10^{-3} M to 10^{-8} M) and added drop wise onto microbeads for the detection. The SERS measurements were performed in Alpha 300 Raman microscope from WITEC using a laser source at 532 nm and with an excitation power of 100 μW. The angle of the light is 90°. All Raman spectra were measured at 20 scans with integration time of 0.1 s over a range from 0 to 3500 cm^{-1}.

2.8. Characterization

Images of scanning electron microscopy (SEM, Quanta 450 SEM; Akishima, Tokyo, Japan) were used to determine to surface morphology and size distribution of the produced microbeads. Energy-dispersive X-ray spectroscopy (EDX, Quanta 450 SEM; Akishima, Tokyo, Japan) and X-Ray Diffraction (XRD, Rigaku, D/Max-2200, USA) data show the surface character of microbeads. Magnetic properties were determined by vibrating sample magnetometer (Cryogenic Limited Model: PPM system, UK) to draw hysteresis curve.

3. Result and discussion

3.1. Characterization of microbeads

The core polymer material, poly (MMES-*co*-GDMA) microbeads were synthesized by a modified seeded polymerization technique *ca*. 5 μm in size, in the monodisperse form. The SEM micrographs showing the size distribution and surface morphology of poly (MMES-*co*-GDMA) microbeads are given in Fig. 1a. As seen here, the microbeads were obtained in the macroporous form. The mean pore size was measured as bidisperse pore size distribution at 20 and 80 nm by inverse-size exclusion chromatography. The specific surface area of polymer microbeads was 39 m^2/g. The carboxyl content of the microbeads was determined as 0.6 mmol/g by potentiometric titration. The chemical route used for the synthesis of SERS substrate is schematically shown in Fig. 2. As seen here, Fe^{2+} and Fe^{3+} cations were adsorbed onto the microbeads via interaction with the anionic carboxyl moiety. To obtain magnetic microbeads, Fe_3O_4 nanoparticles were then in-situ generated within polymeric structure via co-precipitation in basic medium. The microbeads were then further derivatized with APTES to have primary amine functionality on the magnetic beads. Au nanoparticles obtained by citrate reduction were adsorbed onto the amine functionalized magnetic polymer microbeads. In the last stage, Ag nano-shell on the magnetic particles were generated via seed-mediated growth as described in the literature [14]. The SEM photographs of magnetic microbeads are also given in Fig. 1b. As seen here, significant change was observed in the surface morphology of microbeads after magnetization. The SEM photographs showing the surface morphology of Au NP attached and Ag shell containing magnetic polymer microbeads are presented in Fig. 1c and d, respectively. Au NP on the magnetic microbeads were clearly seen type form of white dots on the surface in Fig. 1c. The loading of Ag nanoparticles via seed-mediated growth resulted in a reasonably rough Ag surface on the magnetic microbeads (Fig. 1d).

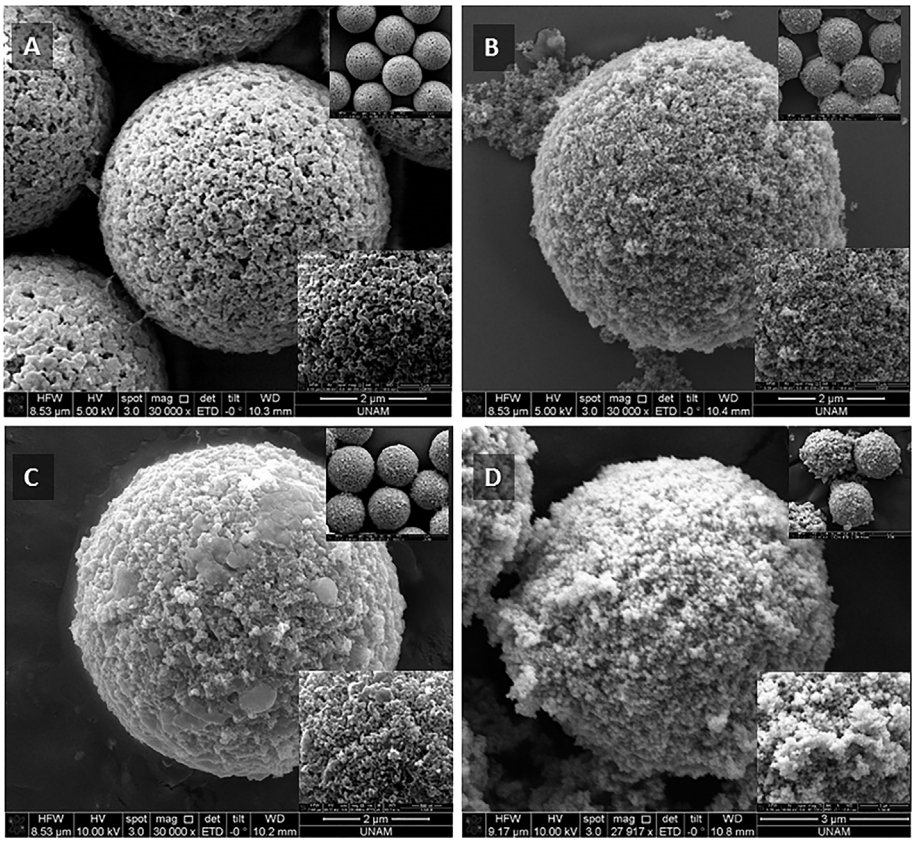

Fig. 1. SEM photos of microbeads (a) Plain poly (MMES-*co*-GDMA) microbeads, (b) Magnetic poly (MMES-*co*-GDMA) microbeads, (c) Gold decorated magnetic poly (MMES-*co*-GDMA) microbeads, (d) Silver coated-magnetic poly (MMES-*co*-GDMA) microbeads.

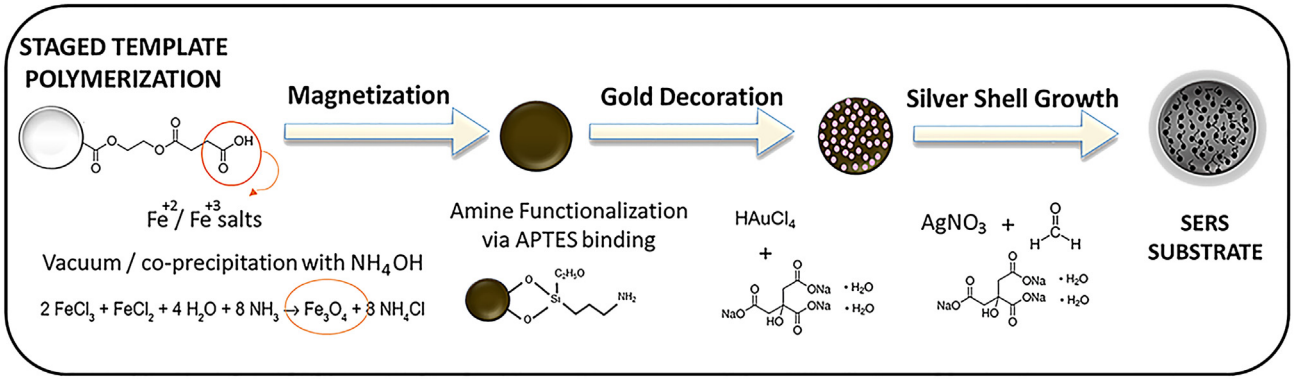

Fig. 2. Represented scheme of chemical route for newly designed SERS substrate synthesis.

The magnetization curves of Ag coated magnetic microbeads are given in Fig. 3 together with the curves given for Au NP coated and bare magnetic microbeads. As seen here, all microbeads type exhibited superparamagnetic behavior. However, the saturation magnetization slightly decreased by the incorporation of Au and Ag NP into the magnetic polymer beads. The SERS platform tried in the presented study is planned for being used in the SERS detection studies involving the specific or pseudo-specific interaction of a ligand functionalized SERS platform with the target molecule to be detected. Following to the interaction with the target molecule in the liquid medium, the separation/isolation of a SERS platform carrying the target molecule, fabricated with the magnetic microspheres will be easier by applying an external magnetic field with a simple magnet. XRD spectra of bare polymer, magnetic polymer, Au coated magnetic polymer and Ag coated magnetic polymer microbeads are given in Fig. 4. Plain poly (MMES-*co*-GDMA) beads had an amorphous structure. The apparent bands observed for Fe_3O_4, Au and Ag were clearly observed the presence of targeted moieties on the corresponding microbeads.

3.2. SERS studies

SERS measurements were done eight times for 1 μl of each sample and repeated on different days to compare obtained SERS spectra. As it was expected there were not many changes recorded peaks and intensities at same conditions. All data were evaluated after background subtraction by using the WITec Project 2.04. The numerical analysis of the peaks was performed using "Originlab" version Originpro8, by including the base-line correction. The trapezoidal integration method was applied for the calculation of peak areas in Fig. 6A and B. The standard deviation was calculated for each data set and took the average of obtained SERS spectra. The characteristic peak areas were analyzed for all measurements.

The SERS active dye, methylene blue was used as model analyte to test the newly designed SERS substrate The SERS spectra obtained with different concentrations of MB on the SERS substrate proposed are given in Fig. 5. As seen here, the intensities of the peaks at 1391, 1436, and 1623 cm^{-1} with their band assignments C—H in-plane ring deformation, C—N asymmetric stretching, C—C ring stretching, respectively were correlated with the MB concentration [37]. The most apparent change was observed for the peak at 1623 cm^{-1}. Fig. 5 showed that the SERS substrate synthesized could be successfully used for the detection of SERS active molecules. The substrate was evaluated for the SERS detection of a member of β-lactam antibiotics, amoxicillin was tried. The SERS spectra obtained with different amoxicillin concentrations on silver coated magnetic polymethacrylate microbeads are given in Fig. 6. As seen here, the intensities of the most apparent peaks 465 cm^{-1} thiazole ring deformation, 620 cm^{-1} bending of —OH, 665 cm^{-1} ring deformation of benzene, 790 cm^{-1} in plane deformation, 865 cm^{-1} benzene ring breathing, 935 cm^{-1} amine bending, 1038 cm^{-1} stretching of amine and C—H, 1171 cm^{-1} C—H bending in benzene ring, 1288 cm^{-1} in plane deformation of benzene,

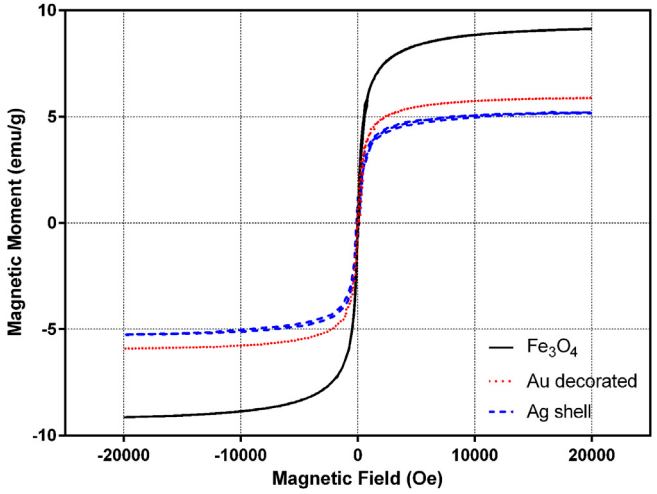

Fig. 3. Magnetic hysteresis curves of microbeads.

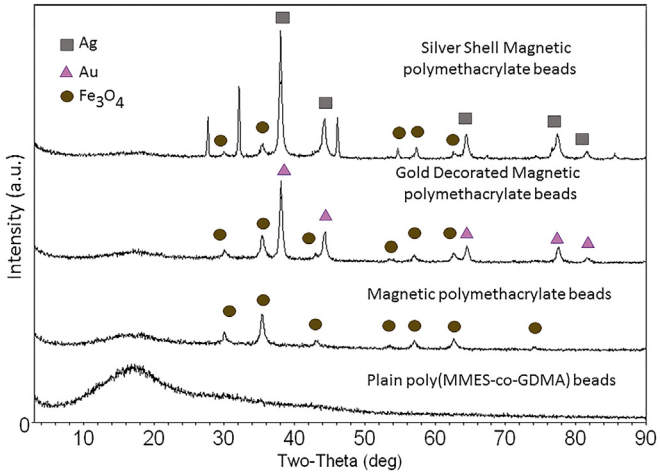

Fig. 4. XRD spectra of synthesized microbeads.

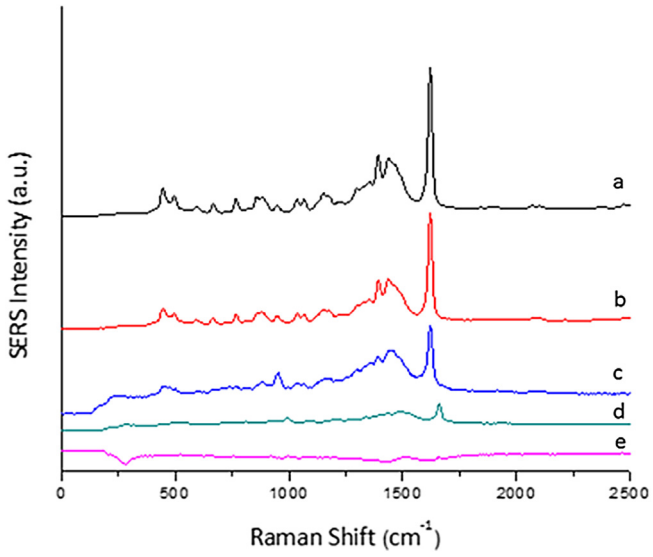

Fig. 5. SERS spectra of methylene blue with different concentrations (M): (a) 10^{-3}, (b) 10^{-4}, (c) 10^{-5}, (d) 10^{-6}, (e) 10^{-7}.

1351 cm^{-1} twisting of amine,1490 cm^{-1} asymmetric bending of CH_3, 1603 cm^{-1} C–C stretching in benzene ring increased with the increasing concentration of amoxicillin in the SERS spectra of amoxicillin [30]. The SERS substrate allowed the detection of amoxicillin up to the concentration of 10^{-8} M. As seen in Fig. 6, the chosen peak areas at 1351, 1171 and 935 cm^{-1} exhibited good linear correlation with the amoxicillin concentration in logarithmic scale that could be used for quantitative determination. Note that eight different SERS spectra from different points in the area formed by the SERS substrate were taken for each sample used in Fig. 6A and B. Then, mean values for the peak areas calculated with respect to eight different SERS spectra taken with the same sample were included with standard deviations.

Largopen (Bilim İlaç Company, Turkey) was included as a real drug to check the SERS behavior of the selected pure antibiotic, amoxicillin. The SERS spectra very similar to those of the active substance were obtained as given in Fig. 6A/B. Then the SERS behaviors of pure amoxicillin and its real drug form, Largopen were compared in Fig. 6A and B. Both the shape characteristics of the peaks and the characteristic Raman shift values were found out very similar both for amoxicillin and its real drug. Hence, the developed SERS platform could be also appropriately used for the low-level detection of commercial drug. The peaks at the same Raman shifts were chosen to express the relationship between peak area and concentration for both real drug and active substance. Good linear correlations with high correlation coefficients between the peak area and the amoxicillin concentration expressed in logarithmic scale were established. The slopes of the calibration curves obtained for active substance and real drug were almost the same (for Fig. 6A and B).

On the other hand, UV-spectrophotometry was selected as a conventional method that could be utilized for the quantitative determination of amoxicillin. The UV spectra obtained with different amoxicillin concentrations and the calibration curve obtained by the evaluation of by UV-spectra are given in Fig. 6C. The calibration curve was constructed by the evaluation of maximum absorbance at 273 nm. As seen here, the lower detection limit of UV-spectrophotometry was 10^{-5} M. By the proposed SERS protocol, amoxicillin could be detected up to 10^{-8} M. Hence, a new analysis protocol based on SERS allowing the detection of selected drug at

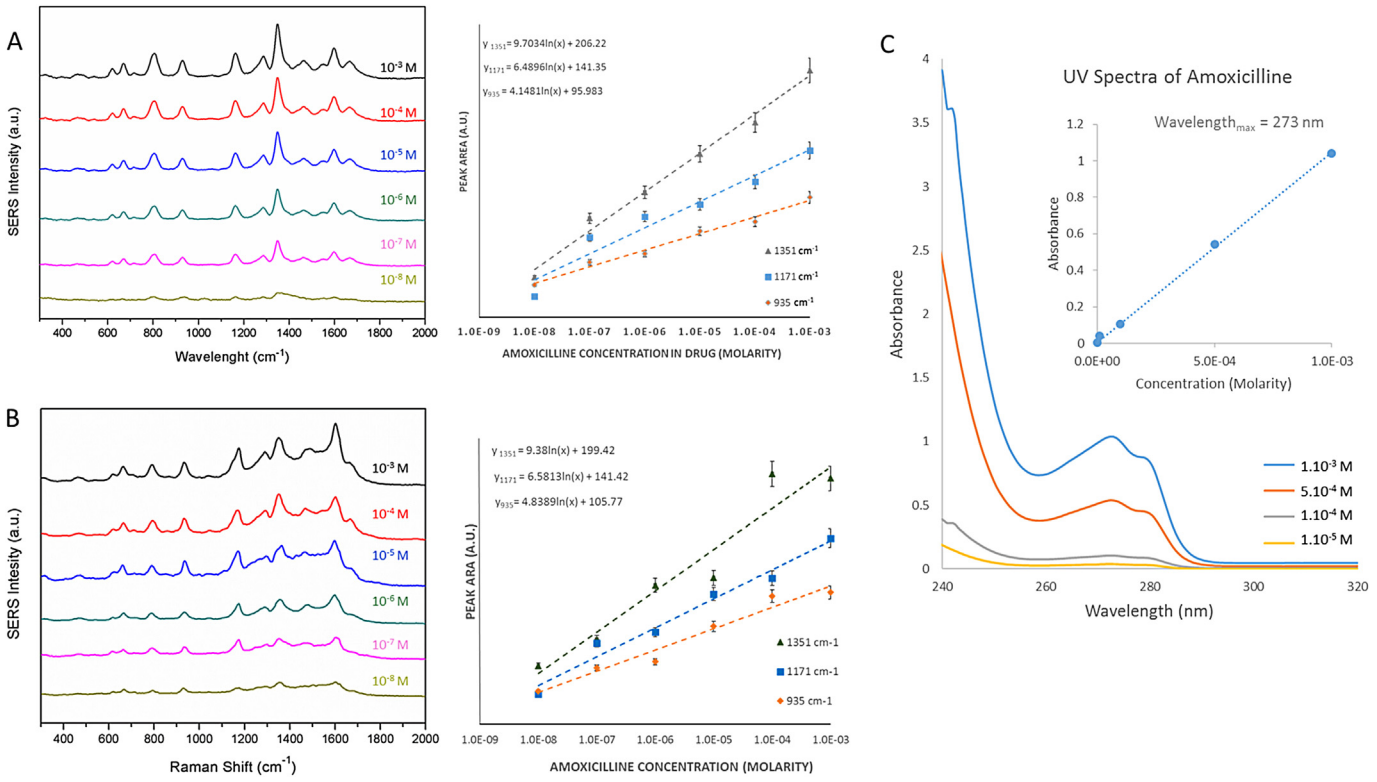

Fig. 6. (A) SERS spectra of commercial amoxicillin (Largopen; Bilim İlaç Company, Turkey) in different concentrations (M) and peak area vs amoxicillin concentration in drug in logarithmic scale, (B) SERS spectra of amoxicillin in different concentrations (M) and peak area vs amoxicillin concentration in logarithmic scale, (C) UV spectra of amoxicillin in different concentration and its calibration curve.

the concentrations 1000 times lower than a conventional method was established.

4. Conclusion

A new SERS platform was synthesized in the form of monodisperse-magnetic polymer microspheres carrying a silver shell. The monodisperse-porous microspheres with carboxyl functionality were synthesized by the multi-stage microsuspension copolymerization. The microspheres were then magnetized by the generation of in-situ formed Fe_3O_4 nanoparticles within the porous structure via a binary precipitation protocol. An Ag shell around the magnetic polymethacrylate microspheres was then generated by a "seed mediated growth protocol". The presence of an Ag shell with roughness in nanometer scale on the magnetic core allowed the use of core–shell microspheres as a suitable platform for SERS detection. Hence, new SERS substrate was evaluated for low-level detection of a chosen antibiotic, amoxicillin. The proposed SERS determination allowed the detection of amoxicillin at trace concentrations up to 10^{-8} M. Then, a amoxicillin assay capable of detecting the selected drug in trace-level *ca*. 1000 times lower than that measured by a conventional spectrophotometric assay was developed. For this reason, the proposed SERS platform can be evaluated as a useful tool for the follow-up amoxicillin pollution and low-level detection of amoxicillin in aqueous media. Additionally, the SERS substrate was designed in the magnetic form by considering the possible potential applications in the future. Because, the magnetic isolation/separation of the SERS substrate functionalized with a ligand specific to the target molecule to be detected in the liquid medium will be easier after specific binding of target antibiotic onto the SERS platform.

References

[1] M. Fleischmann, P.J. Hendra, A. McQuillan, Raman spectra of pyridine adsorbed at a silver electrode, Chem. Phys. Lett. 26 (1974) 163–166.

[2] B. Sharma, R.R. Frontiera, A.-I. Henry, E. Ringe, R.P. Van Duyne, SERS: materials, applications, and the future, Mater. Today 15 (2012) 16–25.

[3] C.M. Doherty, D. Buso, A.J. Hill, S. Furukawa, S. Kitagawa, P. Falcaro, Using functional nano-and microparticles for the preparation of metal–organic framework composites with novel properties, Acc. Chem. Res. 47 (2013) 396–405.

[4] J.-M. Li, W.-F. Ma, C. Wei, L.-J. You, J. Guo, J. Hu, C.-C. Wang, Detecting trace melamine in solution by SERS using Ag nanoparticle coated poly (styrene-co-acrylic acid) nanospheres as novel active substrates, Langmuir 27 (2011) 14539–14544.

[5] C. Feng, Y. Zhao, Y. Jiang, Silver nano-dendritic crystal film: a rapid dehydration SERS substrate of totally new concept, RSC Adv. 5 (2015) 4578–4585.

[6] P. Quaresma, I. Osório, G. Dória, P.A. Carvalho, A. Pereira, J. Langer, J.P. Araújo, I. Pastoriza-Santos, L.M. Liz-Marzán, R. Franco, Star-shaped magnetite@ gold nanoparticles for protein magnetic separation and SERS detection, RSC Adv. 4 (2014) 3659–3667.

[7] Z. Xiaoyan, L. Ruiyi, L. Zaijun, L. Junkang, G. Zhiguo, W. Guangli, A surface-enhanced Raman scattering strategy for detection of peanut allergen Ara h 1 using a bipyramid-shaped gold nanocrystal substrate with an improved synthesis, RSC Adv. 4 (2014) 15363–15370.

[8] M. Yilmaz, E. Senlik, E. Biskin, M.S. Yavuz, U. Tamer, G. Demirel, Combining 3-D plasmonic gold nanorod arrays with colloidal nanoparticles as a versatile concept for reliable, sensitive, and selective molecular detection by SERS, Phys. Chem. Chem. Phys. 16 (2014) 5563–5570.

[9] M. Ranjan, S. Facsko, Anisotropic surface enhanced Raman scattering in nanoparticle and nanowire arrays, Nanotechnology 23 (2012) 485307.

[10] Y. Zhao, W. Zeng, Z. Tao, P. Xiong, Y. Qu, Y. Zhu, Highly sensitive surface-enhanced Raman scattering based on multi-dimensional plasmonic coupling in Au–graphene–Ag hybrids, Chem. Commun. 51 (2015) 866–869.

[11] R. Aroca, R. Alvarez-Puebla, N. Pieczonka, S. Sanchez-Cortez, J. Garcia-Ramos, Surface-enhanced Raman scattering on colloidal nanostructures, Adv. Colloids Interface Sci. 116 (2005) 45–61.

[12] B. Parakhonskiy, Y.I. Svenskaya, A. Yashchenok, H. Fattah, O. Inozemtseva, F. Tessarolo, R. Antolini, D. Gorin, Size controlled hydroxyapatite and calcium carbonate particles: Synthesis and their application as templates for SERS platform, Colloids Surf. B Biointerfaces 118 (2014) 243–248.

[13] I.Y. Stetciura, A.V. Markin, A.N. Ponomarev, A.V. Yakimansky, T.S. Demina, C. Grandfils, D.V. Volodkin, D.A. Gorin, New surface-enhanced Raman scattering platforms: composite calcium carbonate microspheres coated with astralen and silver nanoparticles, Langmuir 29 (2013) 4140–4147.

[14] W. Wang, W. Cai, Y. Yang, H. Li, M. Cong, T. Chen, Controlled growth of metal nanoparticles on amino-functionalized polystyrene microspheres and their application in surface-enhanced Raman spectroscopy, Mater. Chem. Phys. 142 (2013) 756–762.

[15] M. Rycenga, X. Xia, C.H. Moran, F. Zhou, D. Qin, Z.Y. Li, Y. Xia, Generation of hot spots with silver nanocubes for single-molecule detection by surface-enhanced Raman scattering, Angew. Chem. 123 (2011) 5587–5591.

[16] P. Wang, O. Liang, W. Zhang, T. Schroeder, Y.H. Xie, Ultra-sensitive graphene-plasmonic hybrid platform for label-free detection, Adv. Mater. 25 (2013) 4918–4924.

[17] J.-M. Li, W.-F. Ma, L.-J. You, J. Guo, J. Hu, C.-C. Wang, Highly sensitive detection of target ssDNA based on SERS liquid chip using suspended magnetic nanospheres as capturing substrates, Langmuir 29 (2013) 6147–6155.

[18] Y. Wang, K. Wang, B. Zou, T. Gao, X. Zhang, Z. Du, S. Zhou, Magnetic-based silver composite microspheres with nanosheet-assembled shell for effective SERS substrate, J. Mater. Chem. C 1 (2013) 2441–2447.

[19] Z. Guo, L. Chen, H. Lv, Z. Yu, B. Zhao, Magnetic imprinted surface enhanced Raman scattering (MI-SERS) based ultrasensitive detection of ciprofloxacin from a mixed sample, Anal. Methods 6 (2014) 1627–1632.

[20] A. Balzerova, A. Fargasova, Z. Markova, V. Ranc, R. Zboril, magnetically-assisted surface enhanced Raman spectroscopy (MA-SERS) for label-free determination of human immunoglobulin G (IgG) in blood using Fe3O4@ Ag nanocomposite, Anal. Chem. 86 (2014) 11107–11114.

[21] J. Shen, Y. Zhu, X. Yang, J. Zong, C. Li, Multifunctional Fe3O4@ Ag/SiO2/Au core–shell microspheres as a novel SERS-activity label via long-range plasmon coupling, Langmuir 29 (2012) 690–695.

[22] M.H. Shin, W. Hong, Y. Sa, L. Chen, Y.-J. Jung, X. Wang, B. Zhao, Y.M. Jung, Multiple detection of proteins by SERS-based immunoassay with core shell magnetic gold nanoparticles, Vib. Spectrosc. 72 (2014) 44–49.

[23] Q. An, P. Zhang, J.-M. Li, W.-F. Ma, J. Guo, J. Hu, C.-C. Wang, Silver-coated magnetite–carbon core–shell microspheres as substrate-enhanced SERS probes for detection of trace persistent organic pollutants, Nanoscale 4 (2012) 5210–5216.

[24] D.-S. Tira, M. Potara, S. Astilean, Fabrication of stable network-like gold nanostructures in solution and their assessment as efficient NIR-SERS platforms for organic pollutants detection, Mater. Res. Bull. 64 (2015) 267–273.

[25] X.Y. Zhou, R.Y. Li, Z.J. Li, J.K. Liu, Z.G. Gu, G.L. Wang, A surface-enhanced Raman scattering strategy for detection of peanut allergen Ara h 1 using a bipyramid-shaped gold nanocrystal substrate with an improved synthesis, RSC Adv. 4 (2014) 15363–15370.

[26] H. Zhou, D. Yang, N.P. Ivleva, N.E. Mircescu, R. Niessner, C. Haisch, SERS detection of bacteria in water by in situ coating with Ag nanoparticles, Anal. Chem. 86 (2014) 1525–1533.

[27] R. Dong, S. Weng, L. Yang, J. Liu, Detection and direct readout of drugs in human urine using dynamic surface-enhanced Raman spectroscopy and support vector machines, Anal. Chem. 87 (2015) 2937–2944.

[28] K. Wongravee, H. Gatemala, C. Thammacharoen, S. Ekgasit, S. Vantasin, I. Tanabe, Y. Ozaki, Nanoporous silver microstructure for single particle surface-enhanced Raman scattering spectroscopy, RSC Adv. 5 (2015) 1391–1397.

[29] L. He, M. Lin, H. Li, N.J. Kim, Surface-enhanced Raman spectroscopy coupled with dendritic silver nanosubstrate for detection of restricted antibiotics, J. Raman Spectrosc. 41 (2010) 739–744.

[30] A. Bebu, L. Szabó, N. Leopold, C. Berindean, L. David, IR, Raman, SERS and DFT study of amoxicillin, J. Mol. Struct. 993 (2011) 52–56.

[31] K. Herman, L. Szabó, L.F. Leopold, V. Chiş, N. Leopold, In situ laser-induced photochemical silver substrate synthesis and sequential SERS detection in a flow cell, Anal. Bioanal. Chem. 400 (2011) 815–820.

[32] R. Stiufiuc, C. Iacovita, C.M. Lucaciu, G. Stiufiuc, A.G. Dutu, C. Braescu, N. Leopold, SERS-active silver colloids prepared by reduction of silver nitrate with short-chain polyethylene glycol, Nanoscale Res. Lett. 8 (2013) 1–5.

[33] W. Ji, L. Wang, H. Qian, W. Yao, Quantitative analysis of amoxicillin residues in foods by surface-enhanced Raman spectroscopy, Spectrosc. Lett. 47 (2014) 451–457.

[34] B. Elmas, M. Tuncel, G. Yalçın, S. Şenel, A. Tuncel, Synthesis of uniform, fluorescent poly (glycidyl methacrylate) based particles and their characterization by confocal laser scanning microscopy, Colloids Surf. A Physicochem. Eng. Asp. 269 (2005) 125–134.

[35] Z. Ma, Y. Guan, H. Liu, Synthesis and characterization of micron-sized monodisperse superparamagnetic polymer particles with amino groups, J. Polym. Sci. Part A Polym. Chem. 43 (2005) 3433–3439.

[36] G. Schneider, G. Decher, Functional core/shell nanoparticles via layer-by-layer assembly. Investigation of the experimental parameters for controlling particle aggregation and for enhancing dispersion stability, Langmuir 24 (2008) 1778–1789.

[37] M. del Pilar Rodríguez-Torres, L.A. Díaz-Torres, S. Romero-Servin, Heparin assisted photochemical synthesis of gold nanoparticles and their performance as SERS Substrates, Int. J. Mol. Sci. 15 (2014) 19239–19252.